

SHOT NOISE IN DIFFUSIVE SUPERCONDUCTOR/ NORMAL METAL HETEROSTRUCTURES

CHRISTOPH STRUNK

*Institute of experimental and applied physics,
University of Regensburg
Universitätsstr. 31, D-93040 Regensburg, Germany*

AND

CHRISTIAN SCHONENBERGER

*Institute of Physics, University of Basel
Klingelbergstr. 82, CH-4056 Basel, Switzerland*

1. Introduction

According to the scattering theory of quantum transport, the electrons propagate through mesoscopic conductors between large charge reservoirs similar to photons in wave guides. The conductance is described in terms of transmission modes or transport channels with transmission coefficients \mathcal{T}_n . The stochastic transmission of electrical charge through the scattering region causes fluctuations of the current, i.e. current noise. This is called shot noise similar to the noise in vacuum tubes. For a single channel the spectral density $S_I(\omega)$ of the classical shot noise is given by $S_I(0) = 2eI \propto \mathcal{T}$ in the limit of small frequency ω . This result holds for small transmission probabilities $\mathcal{T} \ll 1$ where the statistics of current fluctuations is poissonian. As \mathcal{T} increases the statistics crosses over to a binomial distribution which leads to a suppression of the shot noise $S_I(0) = 2eI(1 - \mathcal{T}) \propto \mathcal{T}(1 - \mathcal{T})$ [1, 2, 3, 4]. In the limit $\mathcal{T} \rightarrow 1$ and temperature $T \rightarrow 0$ the noise vanishes as a consequence of the Pauli principle. At finite temperatures not only the transmission is stochastic, but also the occupation number of the single particle states in the reservoirs. In equilibrium this leads to the thermal (Johnson-Nyquist) noise with $S_I(0) = 4k_B T G$, where G is the conductance of the sample.

On the other hand, the scattering region of a *diffusive* conductor contains usually many transport channels whose transmission coefficients obey

a *universal* distribution function which favors values of \mathcal{T}_n close to zero and close to unity [5]. On average this leads to a universal suppression factor of $1/3$ with respect to the Poisson limit: $S_I(0) = 1/3 \cdot 2eI$ for diffusive wires [6]. This result is universal in the sense, that it does not depend on neither the shape nor the material of the conductor; even spatial variations of the conductivity are allowed [7, 8, 9]. The noise suppression in the diffusive limit has been predicted quite long ago, but was only recently verified experimentally [10, 11]. The reason is related to inelastic scattering of the electrons in the contacts [11], which is hard to treat in the framework of the scattering theory on a quantitative level.

When the electrons can be treated quasi-classically there is an alternative, very different approach to the noise based on the quasiclassical kinetic theory [12, 13]. In this approach the noise is expressed in terms of the quasiclassical distribution function $f(E)$ of the electrons. The binary alternative is the occupation or emptiness of the single particle states rather than the transmission or reflection of electrons. Since $f(E)$ varies between 0 and 1, we have again a binomial distribution. Accordingly, the noise is given by the variance of the occupation number $f(1 - f)$ averaged over energy and space, i.e.:

$$S_I(0) = \frac{4G}{\Omega} \int d^3r dE f(E, x) (1 - f(E, x)) , \quad (1)$$

where Ω is the sample volume.

In this paper we will assume that the samples are narrow wires of length L between large reservoirs, as sketched in Fig. 1a. The main advantage of the kinetic theory is, that it allows the calculation of $f(E)$ via the Boltzmann equation. Taking into account the inelastic scattering it reads in one dimension

$$D \frac{d^2}{dx^2} f(E, x) + \mathcal{I}(E, x) = 0 . \quad (2)$$

Here D is the diffusion constant and \mathcal{I} the collision integral containing $f(E, x)$ and an energy dependent scattering kernel which depends on the nature of the inelastic scattering processes [14]. In the absence of inelastic scattering, $f(E, x)$ varies linearly in space, while for fixed position $f(E, x)$ is a weighted average of the distribution functions in the reservoirs. For a narrow wire at low temperatures $f(E)$ has a two step shape, reflecting the superposition of the two Fermi functions in the reservoirs at each end of the wire. This two-step shape is sketched in Fig. 1b and has recently been observed experimentally [15]. If $f(E, x)$ is inserted into Eq. 1, the $1/3$ -suppression of the shot noise is recovered. The sharpness of the steps is determined by the temperature of the reservoirs. In the presence of inelastic scattering the steps are further smeared until local thermodynamic equilibrium is obtained, i.e. $f(E, x) = f_0(T(x), \mu(x))$, where f_0 is

the fermi function. In this limit, the noise assumes another universal value: $S_I(0) = \sqrt{3}/4 \cdot 2eI$ [12, 16, 17]. We note, that in the absence of inelastic scattering the results of the quasiclassical approach and the scattering approach based on random matrix theories are identical. This holds not only for diffusive wires, but also for chaotic cavities, which are characterized by the universal suppression factor $1/4$ [18, 19, 20].

2. Andreev- and multiple Andreev reflection

Several new features are expected, when one or both of the normal conducting (N) reservoirs are replaced by a superconductor (S). Electrons with energies smaller than the gap energy Δ cannot enter the superconductor because there are no single particle states available. Instead, charge is transferred by the process of Andreev reflection (AR) [21]. An electron with energy E (with respect to the chemical potential of the superconductor) is retroreflected as a hole with energy $-E$ at the NS interface and a Cooper pair enters the superconductor. Since the charge transferred by a single Andreev reflection process is $2e$, the conductance of an ideally transmissive channel doubles [22]. The same doubling is expected for the shot noise of a SNN-structure, where one of the reservoirs is replaced by a superconductor [23]. This has been confirmed experimentally by Jehl *et al.* [24] and by Kozhevnikov *et al.* [25]. As in the NNN-case, the shot noise can be expressed in terms of the kinetic theory [26]. The key point is that a quasiparticle diffusing at an energy $|E| < \Delta$ in the vicinity of the NS-interface hits the interface many times, implying many conversions from electron to hole and vice versa. Because the diffusion times as an electron and as a hole are random, but *equal on average*, one obtains $f(E) = 1/2$ near the NS-interface, provided that the number of electrons impinging from the normal reservoir is equal above and below the chemical potential of the superconductor [27]. The noise calculated with this distribution function is $S_I = 2/3 \cdot 2eI$ in agreement with the naive expectation based on charge doubling. Note, however, that the noise is not generated at the highly transmissive interface (as opposed to the case of tunnel junctions where the noise originates from the barrier), but by the current fluctuations in the diffusive wire. Fig. 3 shows the noise of a diffusive NNS-junction as measured by Jehl *et al.* [28]. The experiment clearly shows the expected shot noise doubling for $eV < \Delta$. The kink at $eV = \Delta$ is caused by the onset of quasiparticle transmission into the reservoirs for $eV > \Delta$. In absence of inelastic scattering, the semiclassical theory agrees again with the quantum theory [23].

If both reservoirs are superconducting, quasiparticles are confined between the two NS-interfaces within an energy range 2Δ . In a naive classical picture the quasiparticles are diffusing back and forth between the two

superconductors, taking Cooper pairs from one side and delivering them on the other. This peculiar 'shuttle' process is called *multiple* Andreev reflection (MAR). A more rigorous quantum mechanical calculation reveals the formation of pairs of Andreev bound states at zero applied voltage [29]. If a phase bias is applied between the superconductors the Andreev bound states carry a net supercurrent at temperatures $k_B T \lesssim E_c$. Here $E_c = \hbar D/L^2$ is the Thouless energy which is determined by the diffusion time τ_D through the sample. In this paper we mainly want to restrict our discussion to the simplest case $k_B T \gg E_c$, where the supercurrent is averaged out. At finite voltages, the MAR manifests itself in a different way. The quasiparticles are no longer confined indefinitely, but can escape after a finite number of Andreev reflections. This is explained in Fig. 2. If the applied voltage eV is an integer fraction of 2Δ , i.e. $n = 2\Delta/eV$, the energy range in which Andreev reflections occur splits up into $n + 1$ branches. For each energy and position along the wire we have both electron- and hole-like quasiparticles arriving from the right, respectively, the left superconductor.

It is essential that the charge transfer q^* per injected quasiparticle increases with the number of Andreev reflections, i.e., $q^* = e(1 + n)$. Hence, a step-like increase of the current at integer fractions of 2Δ is expected, when the bias voltage is reduced. This corresponds to peaks in the differential conductance [30] at voltages $V = 2\Delta/ne$, known as the *subharmonic gap structure*. At low voltage many Andreev reflections are needed, before a quasiparticle can escape into one of the superconducting banks. Subharmonic peaks up to many orders have been observed [31] in ballistic SNS contacts based on InAs quantum wells. The above argument does not depend on whether the quasiparticle motion is ballistic or diffusive and subharmonic gap structures have also been found in diffusive systems [32, 33]. However, since the average diffusion times $\tau_D = L^2/D$ are much longer than the ballistic traversal times $\tau_{ballistic} = L/v_F$, the observation of subharmonic gap structures is more easily hindered by inelastic scattering. An example is shown in Fig. 4, where peaks up to fourth order can be seen. The peak positions scale well with $\Delta(T)$ and $1/n$. Sometimes the peaks are slightly split (i.e. for $n = 3$), a feature not understood yet. Details of the sample design and measurement can be found in [33].

3. Effect of multiple Andreev reflection on the distribution function of diffusive SNS samples

The confinement of quasiparticles by MAR is expected to have a drastic effect on the distribution function. We start the discussion at the high voltage limit and first neglect inelastic scattering. Figure 5 shows a schematic of the distribution function in this limit. If the junction is biased at a high

voltage, e.g., $eV = 4\Delta$, there are two energy regimes where (single) Andreev reflection can occur, i.e., the gap regions of the two superconductors. Since $eV > 2\Delta$ there is an intermediate regime of regular diffusion. As in the NS-case discussed above, the distribution function near the interfaces is reduced to $f(E) = 1/2$, if E is in one of the gap regions. The superposition of these two distributions with equal weight (corresponding to the middle of the wire) results in four steps in $f(E)$ as opposed to the two-step distribution function obtained in the case of normal reservoirs. This peculiar shape of $f(E)$ has been observed directly in a very recent experiment by Pierre *et al.* [34]. Figure 6 shows the evolution of $f(E)$ as a function of voltage. As the bias voltage is reduced the intermediate zone of regular diffusion shrinks and vanishes at $eV = 2\Delta$. For lower voltages the two gap regions overlap and multiple Andreev reflections occur, resulting in even more steps [35]. As the voltage is reduced further, the steps become finer and finer and their number increases. In the limit of $V \rightarrow 0$, $f(E)$ becomes a straight line between 1 at $E = -\Delta$ and 0 at $E = +\Delta$. If $f(E)$ is averaged according to Eq. 1 all step-like features disappear and the noise becomes a straight line [35, 36]:

$$S_I(0) = \frac{2G}{3} (eV + 2\Delta) . \quad (3)$$

This is just the result for a diffusive wire between normal reservoirs, but offset by $4G\Delta/3$. The finite offset of the noise at $V \rightarrow 0$ reflects the finite broadening of $f(E)$ at $V \rightarrow 0$. To compare this result with the Poisson noise it is possible to introduce a voltage dependent Fano-factor defined by

$$S_I(0) = F \cdot 2eI . \quad (4)$$

Comparison with Eq. 3 results in

$$F(V) = \frac{1}{3} \left(1 + \frac{2\Delta}{eV} \right) . \quad (5)$$

This precisely coincides with the naive expectation $S_I(0) = 1/3 \cdot 2q^*I$ with $q^* = e(1 + n)$ and n being the number of Andreev reflections as defined above.

4. Effect of inelastic scattering

The observation that $S_I(0) \rightarrow 4G\Delta/3$ in the limit $V \rightarrow 0$, as evident from Eq. 3, at first sight appears to be in contradiction to the fluctuation dissipation theorem, which states $S_I(0) = 4k_BGT$, i.e., $S_I = 0$ at $T = 0$. This contradiction is resolved in presence of inelastic scattering, when

energy is removed from the electron system. We have to distinguish the effects of inelastic electron-electron (el-el) scattering and electron-phonon (el-ph) scattering. The el-el scattering leads to a smearing of the steps in $f(E)$ towards local thermal equilibrium, including the occupation of states with energies $|E| > \Delta$. In this way a part of the dissipated power can be removed into the reservoirs. The el-ph scattering additionally dumps energy into the bath and thus leads also to a *narrowing* of the distribution function. In real samples, the width of the distribution function will be governed by the balance between the energy input via the current and the energy drain into contacts and the phonon bath, the bottleneck is determined by the energy dependent scattering rates.

In order to calculate the effect of inelastic scattering, the full Boltzmann equation (Eq. 2) has to be solved. This can be done numerically [15]. In Fig. 7 we show $f(E)$ calculated for two examples using Nb (Al) as the superconductor and Au (Cu) as the normal metal. In order to show the effect of different strengths of inelastic scattering we kept the ratio $eV/\Delta = 1.35$ constant in both cases. Because of the much larger gap of Nb ($\Delta_{Nb} \simeq 1.3$ meV) compared to Al ($\Delta_{Al} \simeq 0.186$ meV), the case of Nb involves much higher energies than the case of Al. The scattering integral in Eq. 2 contains a kernel $K(\epsilon)$ depending on the energy exchange ϵ in the collision [37]. The dependence is usually algebraic, i.e. $K(\epsilon) = \kappa \epsilon^\alpha$, where κ is a constant determined by the scattering matrix element and the exponent α is characteristic for the scattering mechanism. For the electron-electron scattering one obtains $\alpha = -3/2$ in the case of disorder enhanced el-el interaction [38] and $\alpha = -2$ in the case of impurity-spin mediated el-el interaction [39]. In contrast, for the el-ph scattering $\alpha = 2$ is found [40], when disorder is neglected. The negative sign of α reflects the importance of quasi-elastic scattering processes characteristic for the el-el interactions [38], while $\alpha = 2$ for the el-ph scattering reflects the energy dependence of the phonon density of states (DOS) in the Debye model. In any case, the collision integral is greatly enhanced with increasing width of the distribution function, because the phase space available for scattering increases. Hence, the scattering is expected to be much more effective in Nb-based junctions as compared to Al-based junctions.

Figure 7a shows $f(E)$ of the Nb based junctions for the three cases of absence of inelastic scattering, inclusion of el-el scattering, and inclusion of both el-el and el-ph scattering. We have used $\alpha_{el-el} = -2$ and values of κ_{el-el} and κ_{el-ph} inferred from weak localization measurements [41]. It is seen that the el-el scattering completely smears the steps expected from independent electron model, while the width of the distribution function is not changed. The inclusion of el-ph scattering leads in addition to a pronounced narrowing of the distribution function, i.e. a cooling of the

electron system by the bath.

On the other hand, for the Al-based junctions the effect of el-el scattering is much less pronounced as illustrated by Fig. 7b. The steps are slightly smeared, but still clearly visible. More important, there is no visible effect of the el-ph scattering. The reason is the rapid decrease of the phonon DOS at low energies. These observations hold nearly unchanged up to $T = 600$ mK.

5. Noise measurements

We now turn to our main experimental results, i.e., the effect of quasiparticle confinement on the shot noise of diffusive SNS junctions. In the case of the Nb-based junctions (see Fig. 8a) we observe a very steep increase (filled circles) of the noise with increasing voltage, which levels off above $V \gtrsim 1$ mV. As a reference, we have also measured the noise in a magnetic field of 6 T, where the superconductivity of the Nb is completely suppressed. In the latter case (open squares) we see the expected linear increase with the $1/3$ suppression factor for diffusive wires. At higher voltages the noise increase with an exponent < 1 , which we attribute to el-ph scattering in the Nb reservoirs [42]. Above $eV = 2\Delta_{Nb}$ the two curves should come very close together because the Andreev reflection rapidly dies out above the gap. This is indeed observed. The solid line is the result of the simulation with no adjustable parameters. The agreement is surprisingly good, because no adjustable parameter has been used. The theoretical curve is nearly independent of κ_{el-el} , but mainly determined by Δ_{Nb} and κ_{el-ph} . Therefore, our measurement demonstrates in particular the cooling of the confined quasiparticles by the el-ph scattering. Similar results have also been obtained by Hoffmann *et al.* [43].

When looking at the Al-based junctions (see Fig. 8b) everything is shifted to much smaller energies. The filled dots are the noise measurements in the superconducting state, showing a roughly linear increase of the noise with the voltage and with an apparently finite intercept on the vertical axis. The open squares represent again the reference measurement in the normal state. In this case the simulation (solid line) does neither depend on κ_{el-el} nor on κ_{el-ph} , but directly reflects Eq. 3, which contains only on Δ_{Al} . This shows that in the investigated voltage range neither the el-el nor the el-ph scattering have an effect on the noise. On the other hand, the simulation and the experimental data agree well only at higher voltages $eV \gtrsim \Delta$. We believe that the apparent suppression of the measured noise with respect to the simple model of incoherent MAR is caused by the proximity effect, which we have neglected so far. This issue will be discussed further in the next section.

6. Multiple charges?

So far we have completely neglected the proximity effect, i.e. the phase coherent propagation of quasiparticles and the Josephson coupling between the superconducting reservoir. At small voltages and our lowest measurement temperature, however, this is not justified, as indicated by the supercurrent apparent in the divergence of the differential conductance near zero bias voltage (see Fig. 4). At $T \simeq 400$ mK the Cooper pairs penetrate into the normal metal on the length scale $L_T = \sqrt{\hbar D / 2\pi k_B T} \simeq 300$ nm. It is plausible that the penetration of the superconducting condensate into the normal wire gives rise to a supercurrent component in the total current which reduces the current noise. In order to check this hypothesis, we have measured the low voltage noise also at elevated temperatures, where the supercurrent is exponentially suppressed. In Fig. 9, we have plotted the Fano factor, respectively the effective charge $q^* = 3e F(V)$ as a function of $1/V$ for different temperatures. The voltage range has been restricted to $V \gtrsim 2 \mu\text{V}$, where the change of the differential conductance dI/dV are kept smaller than 2 to avoid errors when converting the measured voltage noise into current noise. Despite the significant scatter of the data, we see a linear increase of q^* with $1/V$ up to very large values of $q^* \approx 50$ and more. The solid line is the prediction of the semiclassical theory [35, 36], i.e. Eq. 5. The agreement between the semiclassical theory and the data means that even at very low voltages no significant suppression of the shot noise by inelastic processes occurs. The dashed line is the prediction of a fully quantum mechanical calculation by Naveh and Averin [45], which results in a slightly different Fano factor $F = (1 - 1/\sqrt{2}) 2\Delta/eV \simeq 0.29 \cdot 2\Delta/eV$. This is another example for the surprisingly good agreement between quasiclassical and quantum mechanical approaches, although one should keep in mind that the latter calculation is valid in the limit $E_c \gg \Delta$, while our samples are in the opposite limit.

How literally should we take the simple explanation of the enhanced low voltage noise in terms of multiple charges produced by the MAR? Each injected quasiparticle indeed generates a whole avalanche of $2\Delta/eV$ Andreev reflections. Although this process cannot be viewed as the transmission of a coherent charge package, it appears at a single shot in the frequency range where our experiment is operative. We measure at frequencies around 100 kHz, i.e., on the timescale of several microseconds. The diffusion times across our samples are typically fractions of nanoseconds, implying that we cannot detect the correlation times induced by avalanches of 50 MARs and more.

7. Further developments

In this paper we have discussed the simplest possible effects induced by multiple Andreev reflection. However, there are numerous additional effects arising from the proximity effect, which we have completely neglected so far. In a NNS-geometry with one superconducting and one normal reservoir it is known that there are phase coherent contributions to the conductance leading to resistance oscillations in Andreev interferometers [46] and the re-entrance of the proximity-enhanced conductance at low temperatures $k_b T \lesssim E_C$ [47]. The analoga of these phenomena in the noise are discussed by Reulet *et al.* in these proceedings. It is found that the fano factor develops near $eV \simeq E_C$ a phase sensitive suppression below the semiclassical value of $F = 2$ [48].

In SNS-geometries with short wires, the Josephson effects are expected to lead to considerable complications. In fact in the vicinity of the transition to the zero resistance state our samples have exhibited a dramatic supercurrent noise peak [33]. Previous work on shunted Josephson junctions [49] suggests that this may be quantum noise mixed down to lower frequencies. Further work is required to settle this issue and to investigate possible deviations from the RSJ model.

Another very interesting direction of research is the study of extremely small, i.e. *atomic* point contacts as reported by Cuevas *et al.* in these proceedings. Using a mechanical break junction technique, metallic constrictions are prepared which contain only a few conduction channels [50]. The full quantum theory of multiple Andreev reflection is required to describe dc transport and shot noise in atomic dimensions [45, 51, 52]. The quantitative agreement between theory and experiment is excellent [53].

8. Conclusions

We have shown, that the simple effect of quasiparticle confinement by Andreev scattering in diffusive SN- and SNS-junctions has drastic effects on the quasiparticle distribution function. The changes of the distribution function are reflected in the shot noise. When the effect of the inelastic scattering is weak, the noise can mostly be described in terms of an effective charge q^* , introduced by the Andreev reflection. In the case of SNS-junctions, the width of the distribution function at low voltages is finite and of the order of 2Δ , provided that the electron-phonon scattering is weak. On the other hand, when the electron-phonon scattering becomes important, the quasiparticles are thermalized and cooled down. Short Al- and Nb-based junctions are examples for these limiting cases.

Acknowledgements

We thank U. Staufer for providing the Si_3N_4 wafers and T. Hoss, T. Nussbaumer and R. Huber for their contributions to the measurements. In particular, we acknowledge F. Pierre and H. Pothier who provided their simulation program for calculating the distribution functions. We also benefitted from inspiring discussions with C. Bruder, X. Jehl, H. Pothier, M. Sanquer, V. Shumeiko, C. Urbina and B. van Wees. This work was supported by the Swiss National Science Foundation.

References

1. G. B. Lesovik, JETP lett. **49**, 592 (1989).
2. M. Büttiker, Phys. Rev. Lett. **65**, 2901 (1990).
3. M. Reznikov, M. Heiblum, H. Shtrikman, and D. Mahalu, Phys. Rev. Lett. **75**, 3340 (1995).
4. A. Kumar, L. Saminadayar, D. C. Glattli, Y. Jin, and B. Etienne, Phys. Rev. Lett. **76**, 2778 (1996).
5. O. N. Dorokhov, Solid state Comm. **51** 381 (1984).
6. C. W. J. Beenakker and M. Büttiker, Phys. Rev. B **46**, 1889 (1992).
7. Yu. V. Nazarov, Phys. Rev. Lett. **73**, 134 (1994).
8. E. V. Sukhorukov and D. Loss, Phys. Rev. Lett. **80**, 4959 (1998).
9. E. V. Sukhorukov and D. Loss, Phys. Rev. B **59**, 13054 (1999).
10. R. J. Schoelkopf, P. J. Burke, A. A. Kozhevnikov, D. E. Prober, and M. J. Rooks, Phys. Rev. Lett. **78**, 3370 (1997).
11. M. Henny, S. Oberholzer, C. Strunk, and C. Schönenberger, Phys. Rev. B **59**, 2871 (1999).
12. K. E. Nagaev, Phys. Lett. A **169**, 103, (1992).
13. K. E. Nagaev, Phys. Rev. B **52**, 4740 (1995).
14. Here we consider the *angle averaged* distribution function depending only on energy. This is reasonable, because the diffusive motion makes the angle dependent distribution function nearly isotropic.
15. H. Pothier, S. Gueron, N. O. Birge, D. Esteve, and M. Devoret, Phys. Rev. Lett. **79**, 3490 (1997).
16. V. I. Kozub and A. M. Rudin, Phys. Rev. B **52**, 7853 (1995).
17. A. Steinbach, J. M. Martinis, and M. H. Devoret, Phys. Rev. Lett. **76**, 3806 (1996).
18. R. A. Jalabert, J.-L. Pichard, and C. W. J. Beenakker, Europhys. Lett. **27**, 255 (1994).
19. Ya. M. Banter and E. V. Sukhorukov, Phys. Rev. Lett. **84**, 1280 (2000).
20. Phys. Rev. Lett. **86**, 2114 (2001).
21. A. A. Andreev, JETP **19**, 1228 (1964).
22. G. E. Blonder, M. Tinkham, and T. M. Klapwijk, Phys. Rev. B **25**, 4515 (1982).
23. M. J. M. de Jong and C. W. J. Beenakker, Phys. Rev. B **49**, 16070 (1994).
24. X. Jehl, M. Sanquer, R. Calemczuk, and D. Mailly, Nature **405**, 50 (2000).
25. A. A. Kozhevnikov, R. J. Schoelkopf, D. E. Prober, Phys. Rev. Lett., **84**, 3398 (2000).
26. K. E. Nagaev and M. Büttiker, Phys. Rev. B **63**, 081301(R) (2001).
27. This seems trivial in case of one normal and one superconducting reservoir, but is not the case in presence of two superconductors discussed below.
28. X. Jehl and M. Sanquer, Phys. Rev. B **63**, 052511 (2001).
29. I. O. Kulik, Sov. Phys. JETP, **30**, 944 (1973); [Zh. Eksp. Teor. Fiz. **57**, 1745 (1969)].
30. T. M. Klapwijk, G. E. Blonder, and M. Tinkham, Physica **109&110B**, 1657 (1982);

- W. M. van Huffelen *et al.*, Phys. Rev. B **47**, 5170 (1993); A. W. Kleinsasser *et al.*, Phys. Rev. Lett. **72**, 1738 (1994).
31. A. Chrestin, T. Matsuyama, and U. Merkt, Phys. Rev. B **55**, 84578465 (1997).
 32. J. Kutchinsky, R. Taboryski, T. Clausen, C. B. Sørensen, A. Kristensen, P. E. Lindelof, J. Bindslev Hansen, C. Schelde Jacobsen, and J. L. Skov, Phys. Rev. Lett. **78**, 931 (1997).
 33. T. Hoss, C. Strunk, T. Nussbaumer, R. Huber, U. Staufer, and C. Schönenberger, Phys. Rev. B, 4079 (2000).
 34. F. Pierre, A. Anthore, H. Pothier, C. Urbina, and D. Esteve, Phys. Rev. Lett. **86**, 1078 (2001).
 35. K. E. Nagaev, Phys. Rev. Lett. **86**, 3112 (2001).
 36. E. V. Bezuglyi, E. N. Bratus, V. S. Shumeiko, and G. Wendin, Phys. Rev. B **63**, 100501(R) (2001).
 37. F. Pierre, H. Pothier, D. Esteve, and M. Devoret, J. Low. Temp.Phys. **118**, 437 (2000).
 38. For a review, see B. L. Altshuler and A. G. Aronov in *Electron-Electron Interactions in disordered systems*, Edts. A. I. Efros and M. Pollak, Elsevier Science Publishers B. V. (1985).
 39. A. Kaminski and L. I. Glazman, Phys. Rev. Lett. **86**, 2400 (2001).
 40. J. M. Ziman, *Principles of the theory of solids*, Cambridge University Press, Cambridge (1979).
 41. A. B. Gougam, F. Pierre, H. Pothier, D. Esteve, and N. O. Birge, J. Low. Temp.Phys. **118**, 447 (2000).
 42. M. Henny, H. Birk, R. Huber, C. Strunk, A. Bachtold, M. Krüger, and C. Schönenberger, Appl. Phys. Lett. **71**, 773 (1997).
 43. C. Hoffmann, F. Lefloch, and M. Sanquer, cond-mat/0209310.
 44. H. Courtois *et al.*, Phys. Rev. Lett. **76**, 130 (1996).
 45. Y. Naveh and D. V. Averin, Phys. Rev. Lett. **82**, 4090 (1999).
 46. A. Dimoulas, J. P. Heida, B. J. v. Wees, T. M. Klapwijk, W. v. d. Graaf, and G. Borghs, Phys. Rev. Lett. **74**, 602 (1995).
 47. P. Charlat, H. Courtois, Ph. Gandit, D. Mailly, A. F. Volkov, and B. Pannetier, Phys. Rev. Lett. **77**, 4950 (1996).
 48. B. Reulet, A. A. Kozhevnikov, D. E. Prober, W. Belzig, Yu. V. Nazarov, cond-mat/0208089.
 49. C. M. Falco, W. H. Parker, S. E. Trullinger, and P. K. Hansma, Phys. Rev. B **10**, 1865 (1974); R. H. Koch, D. J. Van Harlingen, and J. Clarke, Phys. Rev. B **26**, 74 (1982).
 50. E. Scheer, P. Joyez, D. Esteve, C. Urbina, and M.H. Devoret, Phys. Rev. Lett. **78**, 3535 (1997).
 51. D. Averin and H. Imam, Phys. Rev. Lett. **76**, 3814 (1996).
 52. J. C. Cuevas, A. Martín-Rodero, and A. Levy-Yeyati, Phys. Rev. Lett. **82**, 4086 (1999).
 53. R. Cron, M. F. Goffman, D. Esteve, and C. Urbina, Phys. Rev. Lett. **86**, 4104 (2001).

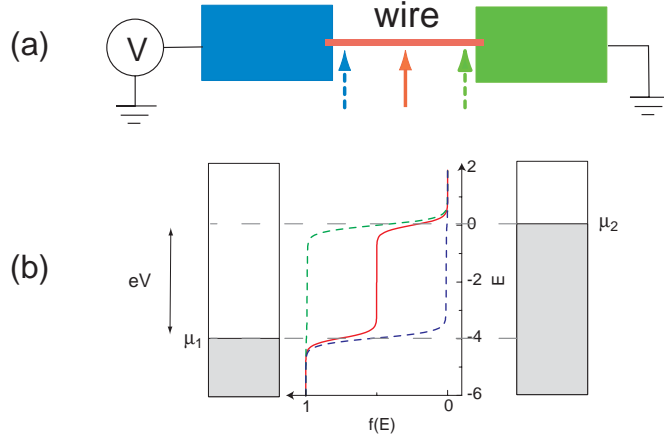


Figure 1. (a) Sketch of a typical sample consisting of a narrow wire made from a diffusive normal metal and two thick and large reservoirs. (b) Schematic of the quasiparticle distribution function near the reservoirs (dashed lines) and in the center of the wire (solid line). In the center a typical two step shape emerges, which results from the superposition of quasiparticles coming from the left and right reservoir.

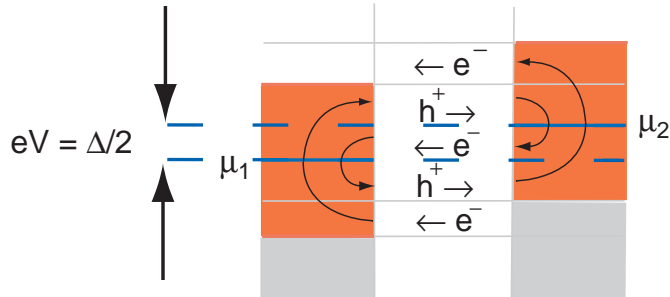


Figure 2. Schematic of the multiple Andreev reflection process for $eV = \Delta/2$. The dark shaded regions correspond to the energy gap. The light shaded regions correspond to occupied quasiparticle states in the superconductors. The electrochemical potential of the two superconductors are labeled μ_1 and μ_2 . Electron-like quasiparticles are injected from the right. Each Andreev reflection at the left interface converts electron-like quasiparticles with energy $-E$ with respect to μ_1 into holes with energy E and vice versa. At the right interface the Andreev reflection takes place with respect to μ_2 . A total charge of $5e$ per quasiparticle is transferred by this particular MAR cycle.

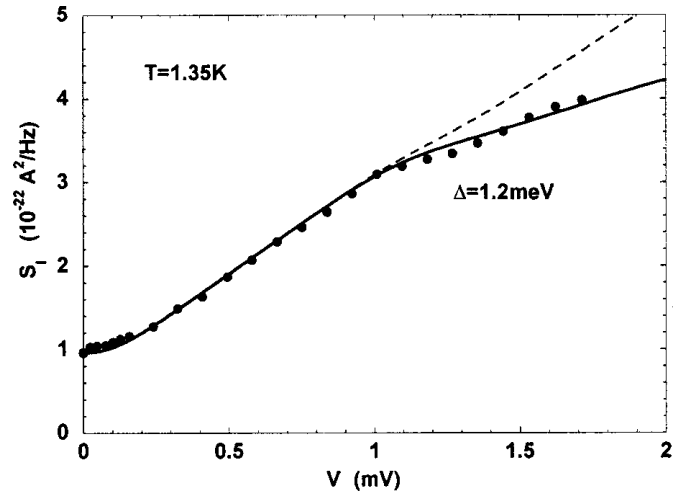


Figure 3. Shot-noise measurements (dots) in an NNS (Cu-Nb) junction compared to the predictions (solid line) from the semiclassical theory [26] with the superconducting gap Δ as only parameter (reproduced from [28]). For $eV < \Delta$ the predicted doubled shot noise is confirmed experimentally. The dashed line simulates a doubled shot noise above Δ to quantitatively emphasize the difference with the normal case. For $eV > \Delta$ an excellent quantitative agreement with the theory is found.

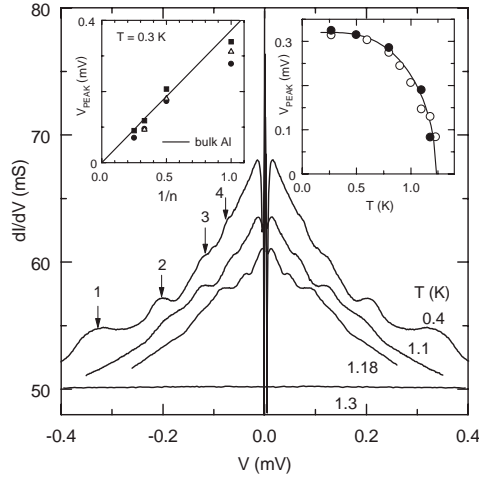


Figure 4. Differential conductance per wire dI/dV vs. voltage V of a chain of 16 Cu wires between Al reservoirs for several temperatures. The Cu wires are $0.9 \mu\text{m}$ long, 160 nm wide and 18 nm thick and have a diffusion constant $D \simeq 72 \text{ cm}^2/\text{s}$. The thickness of the Al reservoirs is 150 nm . The arrows indicate subharmonic gap structures corresponding approximately to integer fractions of 2Δ . The structure at zero bias signals the presence of a supercurrent at the lowest temperatures. Left inset: Position of the conductance peaks vs. $1/n$ for three different samples. The solid line indicates the scaling for the gap of bulk Al. Right inset: Position of the 2Δ conductance peak vs. temperature for two samples with different normal state conductance (\bullet : 50 mS , \circ : 29.3 mS). The solid line is a BCS fit for $2\Delta = 325 \mu\text{eV}$ and $T_c = 1.23 \text{ K}$.

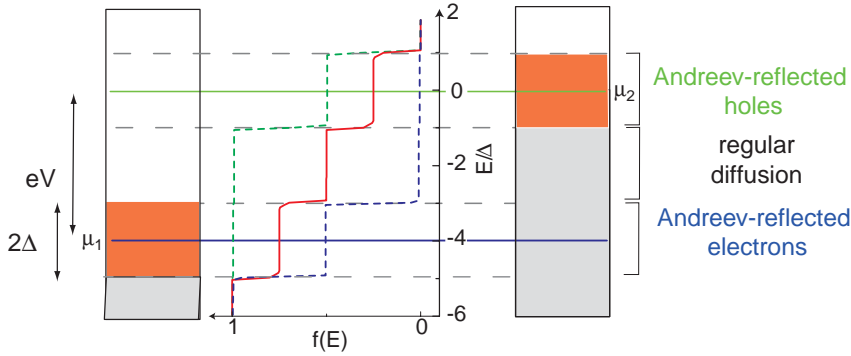


Figure 5. Schematic of the quasiparticle distribution function in an SNS sample at high bias voltage $eV = 4\Delta$. The Andreev reflection in the gap regions of the superconductors near the reservoirs (dashed lines) leads to the generation of holes at the left interface and to the generation of electrons at the right interface. As discussed in the text, $f(E) = 1/2$ in the gap regions. By the superposition of the two boundary functions a four-step shape of the distribution function emerges in the center of the wire (solid line).

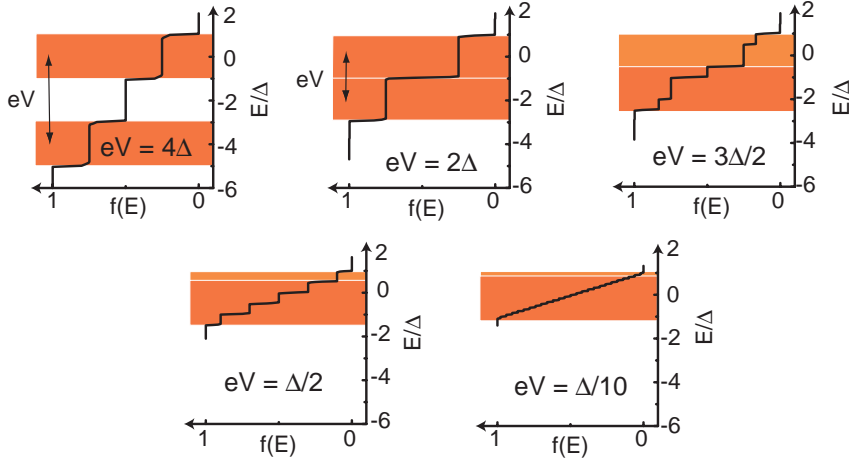


Figure 6. Evolution of the distribution function with decreasing voltage. If the gap regions overlap for $eV < 2\Delta$, multiple Andreev reflections occur. More and more steps appear at low voltages, resulting eventually in a minimal width of the distribution function of 2Δ .

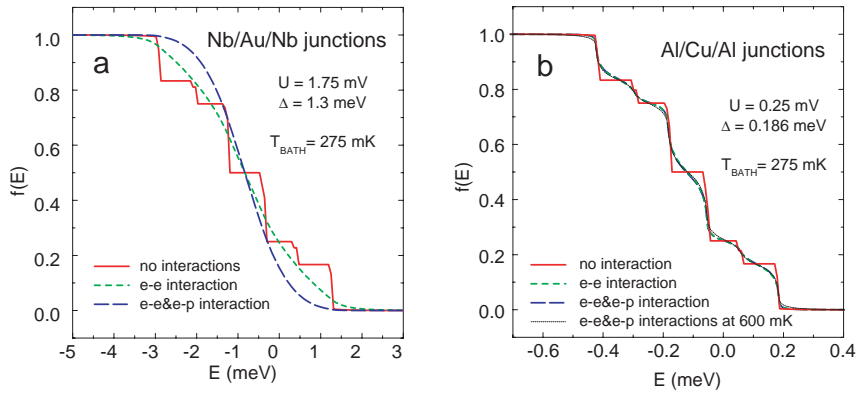


Figure 7. Effect of inelastic scattering on the distribution function of (a) a Nb/Au/Nb contact and (b) a Al/Cu/Al-contact. The ratio $eV/\Delta = 1.35$ is the same in both panels. The figure illustrates the drastic difference in the efficiency of the inelastic scattering on the thermalization and the cooling of the quasiparticles depending on the absolute value of Δ .

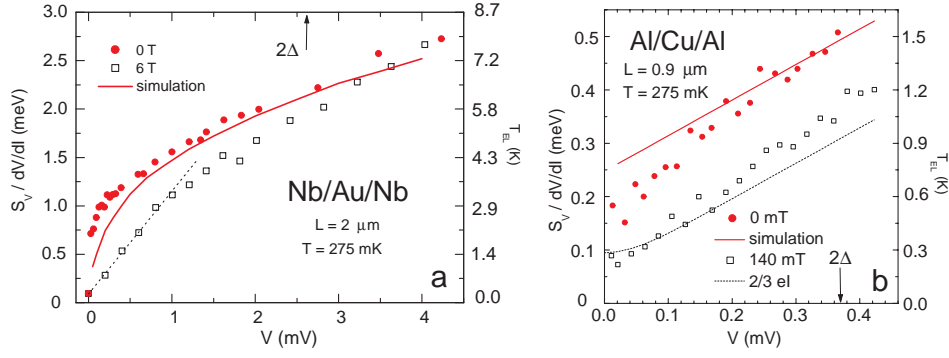


Figure 8. (a) Scaled excess noise $S_V/dV/dI$ as a function of voltage for a series of 9 Nb/Au/Nb junctions of $2 \mu\text{m}$ length, 200 nm width and 15 nm thickness for superconducting (\bullet) and normal (\square) Nb reservoirs. The arrow indicates $V = 2\Delta/e = 2.6 \text{ mV}$. The solid line represents a numerical solution of Eq. 2 assuming for the interaction parameters $\kappa_{el-el} = 4 \text{ ns}^{-1}$, $\kappa_{el-ph} = 13 \text{ ns}^{-1} \text{ meV}^{-3}$ and a diffusion time $\tau_D = 0.56 \text{ ns}$. The dotted line shows the usual 1/3-shot noise suppression for diffusive wires between normal reservoirs. (b) Scaled excess noise $S_V/dV/dI$ as a function of voltage for the same device as in Fig. 4 with superconducting (\bullet) and normal (\square) Al reservoirs. The arrow indicates $V = 2\Delta/e = 0.37 \text{ mV}$. The solid line represents a numerical solution of Eq. 2 assuming for the interaction parameters $\kappa_{el-el} = 1 \text{ ns}^{-1}$, $\kappa_{el-ph} = 5 \text{ ns}^{-1} \text{ meV}^{-3}$ and a diffusion time $\tau_D = 0.11 \text{ ns}$. The dotted line shows the usual 1/3-shot noise suppression for diffusive wires between normal reservoirs.

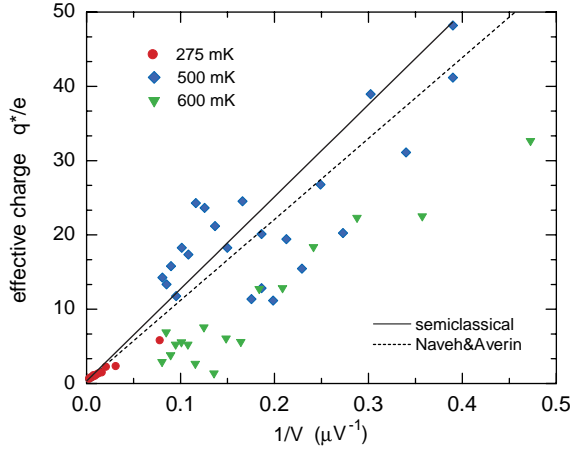


Figure 9. Effective multiple charge $q^* = S_I/2I$ as a function of $1/V$. Despite the considerable scatter of the data, a linear increase of q^* can be seen. The solid line indicates the theoretical estimate for q^* for the quasiclassical theory. The dashed line is the prediction of Naveh and Averin [45].